Photochemical & Photobiological Sciences

PAPER

Check for updates

Cite this: *Photochem. Photobiol. Sci.*, 2019, **18**, 1732

Photochemistry of tyrosine dimer: when an oxidative lesion of proteins is able to photoinduce further damage†

Lara O. Reid,[a] Mariana Vignoni,[a] Nathalie Martins-Froment,[b] Andrés H. Thomas [a] and M. Laura Dántola *[a]

Received 16th April 2019,
Accepted 30th April 2019

DOI: 10.1039/c9pp00182d

rsc.li/pps

The tyrosine dimer (Tyr_2), a covalent bond between two tyrosines (Tyr), is one of the most important modifications of the oxidative damage of proteins. This compound is increasingly used as a marker of aging, stress and pathogenesis. At physiological pH, Tyr_2 is able to absorb radiation at wavelengths significantly present in the solar radiation and artificial sources of light. As a result, when Tyr_2 is formed *in vivo*, a new chromophore appears in the proteins. Despite the biomedical importance of Tyr_2, the information of its photochemical properties is limited due to the drawbacks of its synthesis. Therefore, in this work we demonstrate that at physiological pH, Tyr_2 undergoes oxidation upon UV excitation yielding different products which conserve the dimeric structure. During its photodegradation different reactive oxygen species, like hydrogen peroxide, superoxide anion and singlet oxygen, are produced. Otherwise, we demonstrated that Tyr_2 is able to sensitize the photodegradation of tyrosine. The results presented in this work confirm that Tyr_2 can act as a potential photosensitizer, contributing to the harmful effects of UV-A radiation on biological systems.

Introduction

One of the most important modifications in the oxidative damage of proteins is the covalent bond between two tyrosines (Tyr), yielding the dityrosine cross-link. The one-electron oxidation of Tyr leads to the long-lived tyrosyl radical (Tyr(-H)$^{\bullet}$). The coupling of two Tyr(-H)$^{\bullet}$ yields the dimer *o*,*o*′-dityrosine (Tyr_2, Fig. 1) as the main product.[1] Tyr_2 can be formed photochemically[2,3] or in the dark through reactive oxygen species (ROS) mediated reactions.[4,5] This linkage can occur between two Tyr residues in the same molecule (intramolecular), or between two molecules (intermolecular),[6] the latter leading to high molecular weight products.[7] Tyr_2 is increasingly used as a marker of aging, stress and pathogenesis. It was identified in many pathological manifestations such as amyloid fibril formation, Parkinson's disease, cataract of the eye lens and epidermoid carcinoma.[8]

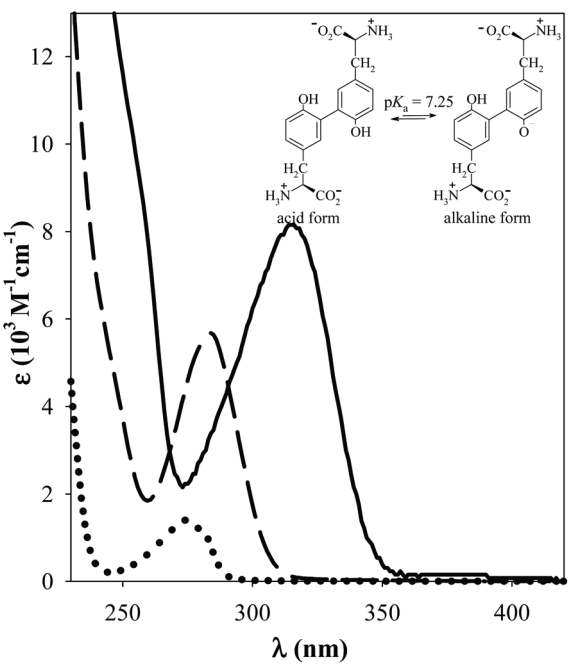

Fig. 1 Absorption spectra of air-equilibrated aqueous solutions of Tyr (dotted line) and, the acid (dashed line) and the alkaline (solid line) forms of Tyr_2. Inset: Acid–base equilibrium in aqueous solutions of Tyr_2.

[a]*Instituto de Investigaciones Fisicoquímicas Teóricas y Aplicadas (INIFTA), Departamento de Química, Facultad de Ciencias Exactas, Universidad Nacional de La Plata, CCT La Plata-CONICET. Casilla de Correo 16, Sucursal 4, (1900) La Plata, Argentina. E-mail: ldantola@inifta.unlp.edu.ar; Fax: +54 221 4254642; Tel: +54 221 4257430 int.153*

[b]*Service Commun de Spectrométrie de Masse (FR2599), Université de Toulouse III (Paul Sabatier), 118, route de Narbonne, F-31062 Toulouse cédex 9, France*

†Electronic supplementary information (ESI) available. See DOI: 10.1039/c9pp00182d

This journal is © The Royal Society of Chemistry and Owner Societies 2019

The phenol groups of Tyr_2 are much more acidic than that of Tyr and the corresponding pK_a value was determined to be 7.25.[9] The two acid–base forms have well differentiated spectral features,[10,11] with absorbance maxima at 283 and 315 nm for the acid and basic form, respectively (Fig. 1). Therefore, in contrast to Tyr, at physiological pH, more than 50% of Tyr_2 exists in the basic form and absorbs in the UV-B (280–320 nm) and UV-A (320–400 nm) spectral regions (Fig. 1). As a result, when Tyr_2 is formed *in vivo* a new chromophore appears in the proteins, which is able to absorb, unlike natural amino acids, at wavelengths significantly present in solar radiation and artificial sources of light.

UV radiation is the most harmful component of solar radiation; the UV-B radiation damages DNA and proteins through the direct excitation of the nucleobases and some amino acids, respectively. However, only a small proportion of the energy that reaches the Earth's surface is UV-B, radiation due to the absorption of the ozone layer in the stratosphere. In addition to direct absorption of light, damage to biomolecules can involve photosensitization reactions, which occur through the absorption of UV-A and/or visible light by endogenous or exogenous photosensitizers. The chemical changes in macromolecules (proteins and DNA) and its components resulting from photosensitized reactions, can take place through different mechanisms: (i) energy transfer from the triplet excited state of the photosensitizer to the biomolecule,[12,13] (ii) photosensitized oxidations, which can take place, through the generation of radicals (Type I mechanism), *e.g.*, *via* electron transfer or hydrogen abstraction, or/and the production of singlet oxygen ($^1O_2$) (Type II mechanism).[14,15] Proteins, due to their relatively high abundance, their ability to bind chromophores and the reactivity of particular amino acid residues, are one of the preferential targets of the damaging effect of radiation on biological systems.[16] It has been reported that different amino acid residues, such as Tyr, histidine (His) and tryptophan (Trp), are chemically modified when proteins are exposed to UV-A or visible light in the presence of a photosensitizer.[7,17–20]

Even though Tyr_2 is one of most common oxidative lesions in proteins, absorbs above 300 nm and can be exposed to UV radiation in different situations, to the best of our knowledge; the photochemistry of Tyr_2 has not been investigated. Therefore, the aim of this work was to find out if Tyr_2 undergoes chemical changes upon UV excitation and if it can act as photosensitizer.

We previously developed a method to synthesize Tyr_2 by the photosensitization of Tyr with pterin (Ptr).[9] Here, we used this method to prepare aqueous solutions of Tyr_2, that afterwards were exposed to UV-B and UV-A radiation to study the photochemistry of the acid and basic forms (Fig. 1). In particular, we have determined the quantum yields of photodegradation, identified the resulting photoproducts and analyzed the kinetics, under different experimental conditions. In addition, we have studied the photosensitizing properties of Tyr_2; in particular, we have investigated the production of ROS and evaluated its capability to act as a photosensitizer using Tyr as target molecule. The results obtained are evaluated in connection with their biological implications.

Material and methods

General

Formic acid (HCOOH), tyrosine (Tyr), deuterium water (D_2O), Cytochrome c (Cyt) from horse heart, and Superoxide Dismutase (SOD) from bovine erythrocytes were obtained from Sigma Aldrich (St Louis, MO). Singlet Oxygen Sensor Green (SOSG) was purchased by Life technologies. Aqueous solutions were prepared using ultrapure water from Milli-Q® purification system (Millipore Corporation, USA).

Preparation of Tyr_2. Tyrosine dimer (Tyr_2) was obtained using the method described in ref. 9. Briefly, air equilibrated aqueous solutions containing Tyr (500 μM) and Ptr (100 μM) were irradiated for 10 min in quartz cells (1.0 cm optical path length) at room temperature using a Rayonet RPR lamp (Southern N. E. Ultraviolet Co.) with emission centered at 350 nm. A liquid chromatography equipment from Shimadzu (see below) and Synergi Polar-RP semi-preparative column (ether-linked phenyl phase with polar endcapping, 250 × 10 mm, 4 μm, Phenomenex) were used for isolation of Tyr_2 from HPLC runs (preparative HPLC), by collecting the mobile phase after passing though the photodiode array detector (PDA). Aqueous solutions (pH 3.0 ± 0.1) were used as mobile phase.[9] The Tyr_2 concentration was determined using Lambert–Beer law ($A^\lambda = \varepsilon^\lambda_{Tyr2} l[Tyr_2]$), using ε^{283}_{Tyr2} = (5680 ± 30) M^{-1} cm^{-1} for the molar extinction coefficient of the acid form.[11]

Measurements of pH. The pH measurements were performed using a pH-meter sensION + pH31 GLP combined with a pH electrode 5010T (Hach) or microelectrode XC161 (Radiometer Analytical). The pH of the aqueous solutions was adjusted by adding drops of HCl and NaOH solutions from a micropipette. The concentration of the acid and the base used for this purpose ranged from 0.1 to 2 M.

UV/Vis analysis. UV/Vis absorption spectra were registered on a Shimadzu UV-1800 spectrophotometer, using quartz cells of 1 cm optical path length.

Steady-state irradiation

Irradiation setup. The continuous irradiation of aqueous solutions of Tyr_2 at different pH (5.5 ± 0.1 and 9.5 ± 0.1) was carried out at room temperature. The samples (1 mL) were photolyzed in quartz cell (4 mm optical path length) using an irradiation setup (Newport) composed by a Xenon Lamp (300 W), coupled, through a Mounting Kit (Model 74017), to a motorized monochromator UV-VIS (Oriel Cornerstone 130 1/8 m). The acid and basic forms of Tyr_2 were irradiated at (280 ± 20) nm and (320 ± 20) nm, respectively. The experiments were performed in the presence and in the absence of dissolved O_2. Experiments with air-equilibrated solutions were carried out in open quartz cells without bubbling, whereas argon and oxygen-saturated solutions were obtained by bub-

bling for 20 min with these gases, previously water saturated (Linde, purity >99.998%).

Actinometry. Aberchrome 540 (Aberchromics Ltd) was used as an actinometer for the measurement of the incident photon flux densitity ($q^{0,V}_{n,p}$) at the excitation wavelength, which is the amount of incident photons per time interval ($q^{0}_{n,p}$) and divided by the volume (V) of the sample.[21] Aberchrome 540 is the anhydride form of the (*E*)-α-(2,5-dimethyl-3-furylethylidene)(isopropylidene)succinic acid which, under irradiation in the spectral range 316–366 nm leads to a cyclized form. The method for the determination of $q^{0,V}_{n,p}$ has been described in detail.[22] A value of 1.4 (±0.1) × 10^{-6} Einstein per L per s was obtained for $q^{0,V}_{n,p}$ at 320 nm. The value of the absorbed photon flux density ($q^{a,V}_{n,p}$) was calculated from $q^{0,V}_{n,p}$ according to the Lambert–Beer law:

$$q^{a,V}_{n,p} = q^{0,V}_{n,p}(1 - 10^{-A}) \quad (1)$$

where A is the absorbance of the reactant at the excitation wavelength.

Taking into account that Aberchrome cannot be used to determine the $q^{0,V}_{n,p}$ at 280 nm, the $q^{0,V}_{n,p}$ value was calculated using the following equation:

$$q^{0,V}_{n,p}(280) = q^{0,V}_{n,p}(320)\frac{I(280)}{I(320)} \quad (2)$$

where $q^{0,V}_{n,p}$ (280) and $q^{0,V}_{n,p}$ (320) are the $q^{0,V}_{n,p}$ values at 280 nm and 320 nm, respectively and I(280) and I(320) are the emission intensities of the irradiation setup at 280 nm and at 320 nm, respectively. To determine I(280)/I(320) the corresponding emission spectra at the monochromator output were registered with an Ocean Optics SD 2000 spectrometer.

Chromatographic analysis

High-performance liquid chromatography (HPLC). A Prominence equipment from Shimadzu (solvent delivery module LC-20AT, on-line degasser DGU-20A5, communications bus module CBM-20, auto sampler SIL-20A HT, column oven CTO-10AS VP, photodiode array (PDA) detector SPD-M20A and fluorescence (FL) detector RF-20A) was employed. The samples before and after irradiation were analyzed using both detectors connected in series (HPLC-PDA and HPLC-FL analyses). A Synergi Polar-RP analytical column (ether-linked phenyl phase with polar endcapping, 150 × 4.6 mm, 4 μm, Phenomenex) was used for separation. Solutions containing 100% HCOOH (25 mM, pH 3.3 ± 0.1) were used as mobile phase; at this pH only the acid form of Tyr_2 is present.

Mass spectrometry analysis. The liquid chromatography equipment coupled to mass spectrometry (LC-MS) system was equipped with an UPLC chromatograph (ACQUITY UPLC, Waters), and a UV/vis detector (Acquity TUV), coupled to a quadrupole time-of-flight mass spectrometer (Xevo G2-QTof-MS, Waters) (UPLC-QTof-MS), equipped with an electrospray ionization source (ESI). UPLC analyses were performed using the Acquity UPLC BEH Phenyl (1.7 μm, 2.1 × 50 mm) column (Waters). An isocratic elution with 99% of aqueous HCOOH (0.1% v/v) and 1% of ACN was used as mobile phase with a flow rate of 0.2 mL min^{-1}. Mass chromatograms, *i.e.* representations of mass spectrometry data as chromatograms (the *x*-axis representing time and the *y*-axis signal intensity), were registered using different scan ranges. The mass spectrometer was operated in both positive (ESI^+) and negative (ESI^-) ion modes. When solutions of pure Tyr_2 were analyzed, the signal corresponding to the intact molecular ion was observed in the sample stored in dark and after irradiation; new signals were detected and allowed the identification of different photoproducts. Given that the signals were obtained with better resolution in ESI^- mode, the mass spectrometry analyses were carried out in this mode.

Reactive oxygen species

Hydrogen peroxide (H_2O_2). For the determination of H_2O_2, a Cholesterol Kit (Wiener Laboratorios S.A.I.C.) was used. H_2O_2 was quantified after reaction with 4-aminophenazone and phenol.[23,24] Briefly, 500 μL of irradiated solution were added to 600 μL of reagent. The absorbance at 505 nm of the resulting mixture was measured after 30 min of incubation at room temperature, using the reagent as a blank. Aqueous H_2O_2 solutions prepared from commercial standards were employed for calibration.

Superoxide anion radical ($O_2^{\bullet-}$). The $O_2^{\bullet-}$ was detected using the SOD-inhibitable Cyt reduction assay.[25] Solutions of Tyr_2 were irradiated in the presence of 14 μM Cyt. The extent of Cyt reduction was determined by monitoring the increase in the absorbance at 550 nm. The absorption spectra of oxidized and reduced Cyt are very characteristic, and this spectral change is a sensitive assay for electron-transfer reactions.

Singlet oxygen ($^1O_2$) detection. For $^1O_2$ detection the experiments were carried out at room temperature using deuterium water as a solvent since the lifetime of $^1O_2$ (τ_Δ) is long enough to detect it. The $^1O_2$ emission in the near-infrared (NIR) region was registered using a NIR PMT Module H10330-45 (Hamamatsu) coupled to a single-photon counting equipment FL3TCSPC-SP, as described elsewhere.[26] Briefly, the sample solution (0.7 mL) in a quartz cell (1 cm × 0.4 cm) was irradiated with a CW 450 W Xenon source through an excitation monochromator (330 nm blaze grating). The luminescence in the NIR region, after passing through an emission monochromator (1000 nm blaze grating), was detected at 90° with respect to the incident beam. Corrected emission spectra obtained by excitation at 320 nm were recorded between 950 and 1400 nm.

Singlet oxygen quantum yields (Φ_Δ). The probe Singlet Oxygen Sensor Green (SOSG) was used to determine the Φ_Δ. When SOSG reacts with $^1O_2$ produces an endoperoxide (SOSG-EP) that shows a typical fluorescence in the visible region.[27–29] Air equilibrated aqueous solutions of Tyr_2 (A = 0.12 at 320 nm) were irradiated in the presence of 0.63 mg L^{-1} of SOSG. The SOSG-EP formed as a function of irradiation time, was detected by its fluorescence with maximum emission at 525 nm upon 470 nm excitation. To quantify $^1O_2$ in these experiments, the 525 nm emission was determined using

 This journal is © The Royal Society of Chemistry and Owner Societies 2019

Pterin (Ptr) as a reference of $^1O_2$ sensitizer (Φ_Δ = 0.30).[30] For determining Φ_Δ of Tyr_2, the initial rate of SOSG-EP production ($(d[SOSG\text{-}EP]/dt)_0$) of air equilibrated aqueous solution of Tyr_2 and Ptr were alternatively measured, using matched absorbances at the wavelength(s) of excitation. The Φ_Δ of Tyr_2 was calculated using the following equation:

$$\Phi_{\Delta,Tyr2} = \frac{\left(\frac{d[SOSG\text{-}EP]}{dt}\right)_{0,Tyr2}}{\left(\frac{d[SOSG\text{-}EP]}{dt}\right)_{0,Ptr}} \Phi_{\Delta,Ptr} \quad (3)$$

where $(d[SOSG\text{-}EP]/dt)_{0,Tyr2}$ and $(d[SOSG\text{-}EP]/dt)_{0,Ptr}$ are the initial rate of SOSG-EP production of air equilibrated aqueous solution of Tyr_2 and Ptr, respectively and $\Phi_{\Delta,Ptr}$ is the quantum yield of $^1O_2$ production by Ptr.

Quantum yield of Tyr_2 consumption

The quantum yield of Tyr_2 consumption (Φ_{-Tyr2}) was determined for the acid and basic form of Tyr_2 at 280 and 320 nm, respectively. Values were obtained using eqn (4).

$$\Phi_{-Tyr2} = \frac{\left(-\frac{d[Tyr2]}{dt}\right)_0}{q^{a,V}_{n,p}} \quad (4)$$

with $(-d[Tyr_2]/dt)_0$: initial rate of Tyr_2 consumption and $q^{a,V}_{n,p}$: photon flux absorbed by the reactant (eqn (1)).

The initial rates were obtained from the slopes of the corresponding plots of Tyr_2 concentration *vs.* time at acid and alkaline pH. The evolution of Tyr_2 during irradiation was followed by HPLC-FL, using the characteristic emission properties of Tyr_2 at 410 nm when the sample is excited at 280 nm.

Results and discussion

Photodegradation of Tyr_2 in aqueous solutions

The first aim of this work was to find out if Tyr_2 was able to suffer degradation in aqueous solutions upon UV irradiation. Therefore acidic (pH = 5.5 ± 0.1) and alkaline (pH = 9.5 ± 0.1) air-equilibrated aqueous solutions of Tyr_2 were irradiated at 280 and 320 nm, respectively. Significant changes in the absorption spectra of the alkaline solutions were registered upon irradiation (Fig. 2a). In particular, decrease of the intensity of the bands corresponding to the reactant and an increase of the absorbance at wavelengths longer than 350 nm was observed (Fig. 2a). In contrast, very small spectral changes were registered for the photolysis of the acid form of Tyr_2 (Fig. 2b). No further spectral changes were detected for irradiated solutions stored in the dark for several hours.

Chromatograms obtained by HPLC-FL analysis of irradiated oxygen-free, air-equilibrated and oxygen-saturated solutions (excitation at 280 nm and emission at 410 nm) showed that Tyr_2 suffers photodegradation in the presence of oxygen (Fig. 2). In the experiments lacking oxygen, the Tyr_2 concentration remained constant and no photoproducts were detected, which indicates that the photochemical degradation of Tyr_2 is a photooxidation process. On the other hand, no significant differences in the consumption of Tyr_2 were found in oxygen-saturated in comparison with air-equilibrated solution.

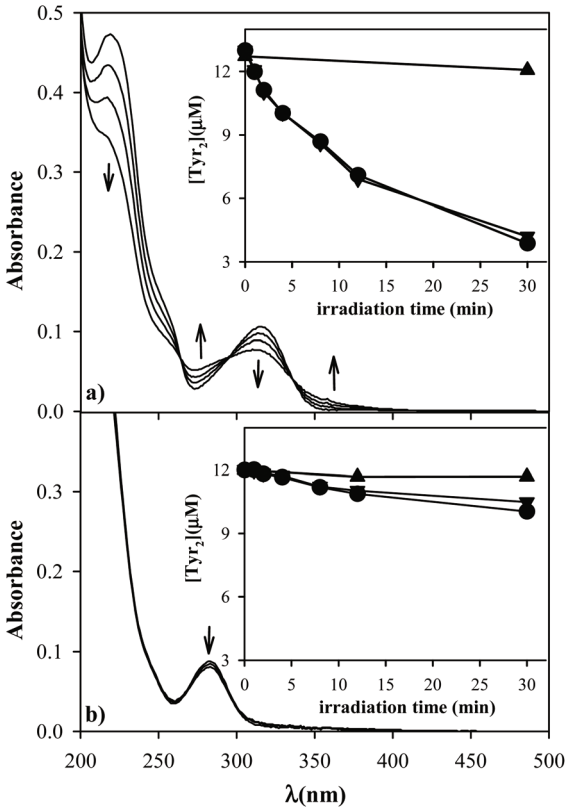

Fig. 2 Evolution of the absorption spectra of air equilibrated aqueous solution of Tyr_2 at (a) pH 9.5 and (b) pH 5.5, as a function of irradiation time. Inset: Time evolution of Tyr_2 concentration, calculated from HPLC analysis (FL detector, excitation at 280 nm, emission at 410 nm), in air-equilibrated (●), oxygen-saturated (▼) and oxygen-free (▲) aqueous solutions at (a) pH 9.5 and (b) pH 5.5.

The quantum yield of Tyr_2 consumption (Φ_{-Tyr2}) was determined in air-equilibrated acidic and alkaline solutions (eqn (4), Material and methods). For determining the initial rates of Tyr_2 consumption ($(-d[Tyr_2]/dt)_0$), the plots of concentration *vs.* irradiation time must be linear. Generally, this condition is fulfilled only if the absorbed photon flux density ($q^{a,V}_{n,p}$) by the reactant does not decrease significantly (<15%). Therefore, for each experiment it was considered a period of time, within this condition was satisfied. We took into account only the first 20 minutes for acidic media and 10 minutes for alkaline media. The Φ_{-Tyr2} values obtained for air-equilibrated aqueous solution of Tyr_2 were 0.023 ± 0.003 and 0.0053 ± 0.0005 for the alkaline and acid form, respectively. Considering that these values are higher than those reported for Tyr,[31] which, in addition, does not absorb UV-A radiation, it is clear that at physiological conditions, Tyr_2 is able to suffer photodegradation much easier than Tyr.

These results demonstrated that Tyr_2 undergoes degradation upon UV-A irradiation. Since UV-A is the most important UV component of solar radiation and considering that the intensity of our light source is not higher than that of solar radiation,[32] the photochemistry of Tyr_2 becomes relevant and deserves to be studied. Moreover, the quantum yields measured are relatively high, which implicates that the photochemical reaction can be significant even upon exposure in short periods of time and with radiation of low energy.

Analysis of photoproducts

To investigate the products of the photodegradation of Tyr_2, the irradiated solutions were analyzed by HPLC-PDA and HPLC-FL (Material and methods). The HPLC-PDA analysis showed that Tyr_2 photodegradation in alkaline media led to the formation of many products (Fig. 3). Although noisy, the spectra of three photoproducts, arbitrary named P1, P2 and P3, were recorded (Fig. 3). The photoproduct P3 showed spectral features similar to those reported for the typical oxidation products of Tyr *in vivo*, dopaminochrome or dopachrome.[33]

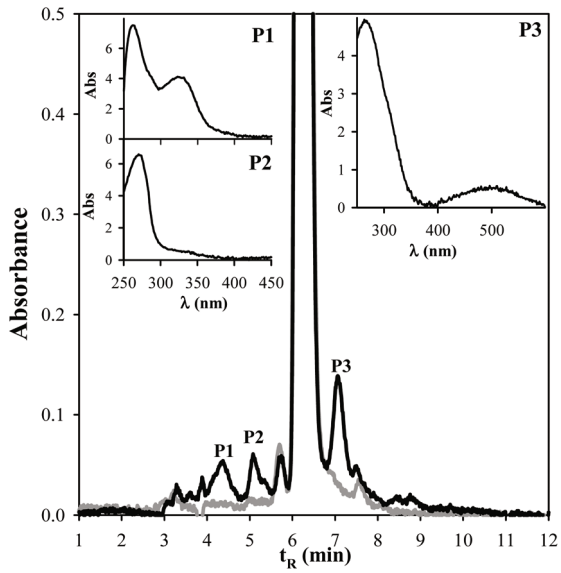

Fig. 3 Chromatograms obtained in HPLC-PDA analysis at 280 nm of Tyr_2 before (gray line) and after 10 min (black line) of irradiation. Insets: Absorption spectra of the main photoproducts. $[Tyr_2]_0$ = 43 μM, pH = 9.5.

The absorption spectra of these compounds have a broad absorption band of low intensity centered on 475 nm. These compounds are formed by an irreversible intramolecular cyclization of 3,4-dihydroxy-L-phenylalanine (DOPA), which suggests the formation of DOPA as a photoproduct of Tyr_2.[33]

In addition, Tyr was searched among the products using a standard solution and the characteristic fluorescence features of the amino acid.[34] The chromatograms obtained by HPLC-FL analysis (λ_{exc} = 275 nm, λ_{em} = 300 nm) revealed that Tyr was not a product of Tyr_2 photodegradation, indicating that the dimerization process cannot be reverted photochemically by direct excitation of Tyr_2.

To gain insight on the structural characteristics of the products formed by the photodegradation of Tyr_2, a qualitative analysis of these compounds was carried out by liquid chromatography/mass spectrometry using a UPLC equipment coupled to a mass spectrometer (UPLC-QTof-MS, Material and methods). Before irradiation the chromatograms showed a main peak, and the mass spectrum recorded for this peak exhibited the signal corresponding to the intact molecular ion of Tyr_2 as $[M - H]^-$ species at m/z 359.1237 (M : Tyr_2) (Table 1).

After the irradiation, several new peaks were observed in the chromatograms. The mass spectra recorded at different retention times (t_R) revealed, at least, four products with m/z values higher than that of Tyr_2 (Table 1) which corresponded to compounds that have incorporated one ([M + O], [M + O − 2H]) or two oxygen atoms ([M + 2O], [M + 2O − 2H]). Incorporation of one oxygen atom ([M + O]) suggested the oxidation of one unit of Tyr to DOPA, a common oxidation product of Tyr.[35] Incorporation of one oxygen atom and the loss of two hydrogen atoms ([M + O − 2H]) suggested the oxidation of one unit of Tyr to dopaquinone, another common oxidation product of Tyr.[33] Therefore we propose that the four mentioned products are dimeric structures composed by a Tyr unit and an oxidized Tyr unit, or two oxidized Tyr units (Fig. 4).

Furthermore, UPLC-QTof-MS analysis also revealed the formation of products of molecular weights lower than that of the reactant. In particular, an intense signal was detected for m/z value of 327.0984 (Table 1). Taking into account that the intramolecular cyclization of quinone is a commun reaction,[33] the structure of this product could be a dimeric structure formed by a Tyr and a dopaminochrome (Fig. 4). This proposed structure justifies the absorbance in the visible region observed for

Table 1 Molecular formula, observed and calculated mass and mass error of Tyr_2 and oxidized products detected in LC-MS spectra

Compound	[M]	Elemental composition	ESI^- $[M - H]^-$		
			Observed (m/z)	Calculated (m/z)	Error (ppm)
Tyr_2	Tyr_2	$C_{18}H_{20}N_2O_6$	359.1237	359.1249	−3.3
Tyr-DOPA	Tyr_2 + O	$C_{18}H_{20}N_2O_7$	375.1182	375.1198	−4.3
Tyr-dopaquinone	Tyr_2 + O–2H	$C_{18}H_{18}N_2O_7$	373.1027	373.1041	−3.8
DOPA-DOPA	Tyr_2 + 2O	$C_{18}H_{20}N_2O_8$	391.1128	391.1147	−4.9
DOPA-dopaquinone	Tyr_2 + 2O–2H	$C_{18}H_{18}N_2O_8$	389.0976	389.0990	−3.6
Tyr-dopaminochrome	Tyr_2 + O–2H–HCOOH	$C_{17}H_{16}N_2O_5$	327.0984	327.0986	−0.6

This journal is © The Royal Society of Chemistry and Owner Societies 2019

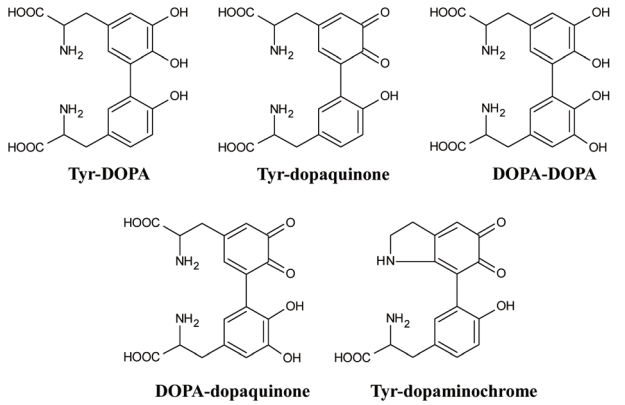

Fig. 4 Proposed molecular structure for the oxidized products detected in LC-MS analysis of alkaline aqueous solution of Tyr_2 exposed to UV-A radiation.

P3 in the HPLC-PDA chromatograms (Fig. 3). In agreement with the previous results of HPLC-FL analysis, Tyr was not found as a product of photodegradation of Tyr_2.

The UPLC-QTof-MS equipment was used for tandem mass spectrometry (MS/MS) analysis. MS/MS spectra registered for Tyr_2 at different ionization energies showed the loss of different fragments of the side chains (Fig. 5). In contrast, the fragmentation did not involve the aromatic rings, which indicated that the bond between the two Tyr residues is strong enough to not be broken under our experimental conditions. This type of fragmentation pattern has already been observed for DOPA.[36]

Due to the low concentration, most of the MS/MS spectra of the products were noisy with weak signals. However, in all cases it was observed that the fragmentation took place in the side chains and not in the rings. Fig. S1 (ESI†) shows the MS/MS spectrum registered for Tyr-DOPA, where a fragmentation pattern similar to that observed for Tyr_2 (Fig. 5) can be appreciated. The MS/MS spectrum of Tyr-DOPA confirmed that the incorporation of the oxygen atom takes place in one of the aromatic rings. In the case of Tyr-dopaminochrome, its MS/MS spectrum (Fig. S2, ESI†) showed the fragmentation of Tyr_2 in only one of the two side chains, supporting the hypothesis that the other chain is involved in the cyclization.

In overview, the results presented in this section showed that the photodegradation of Tyr_2 under UV-A radiation involves the oxidation of the aromatic ring of the chemical structure of Tyr, which leads to many dimers bearing the common oxidation products of Tyr such as DOPA and dopaquinone and colored cyclized compounds. In all the cases, the products conserve the dimeric structure, indicating that once Tyr_2 is formed, it undergoes photooxidation upon UV-A irradiation, but the chemical bond between the two Tyr moieties remains unaltered.

Production of reactive oxygen species

Aromatic amino acids, like Trp and Tyr, are able to produce ROS by direct light absorption[37] or by photosensitization reaction induced by endogenous or exogenous photosensitizers.[17,18] We have demonstrated in the previous section that excitation of Tyr_2 with UV-A and UV-B radiation generates electronic excited states that initiate photoreactions. Therefore it is straightforward to think that Tyr_2 might also produce ROS photochemically, which would be relevant since Tyr_2 can be excited at longer wavelengths than Tyr and other aromatic amino acids. Consequently the production of H_2O_2, $O_2^{\bullet-}$ and $^1O_2$ was evaluated in air-equilibrated aqueous solutions of Tyr_2 exposed to UV radiation.

Hydrogen peroxide determination. In alkaline Tyr_2 solutions (14 μM, pH = 9.5), H_2O_2 was formed and the concentration increased as a function of irradiation time (Fig. 6). The H_2O_2 production was compared to the consumption of Tyr_2 ($\Delta[Tyr_2] = [Tyr_2]_0 - [Tyr_2]_t$), simultaneously determined by HPLC. The results indicated that the amount of H_2O_2 produced was equal, within experimental error, to the consumption of Tyr_2. This fact suggests that H_2O_2 is formed as a product of the photooxidation of Tyr_2.

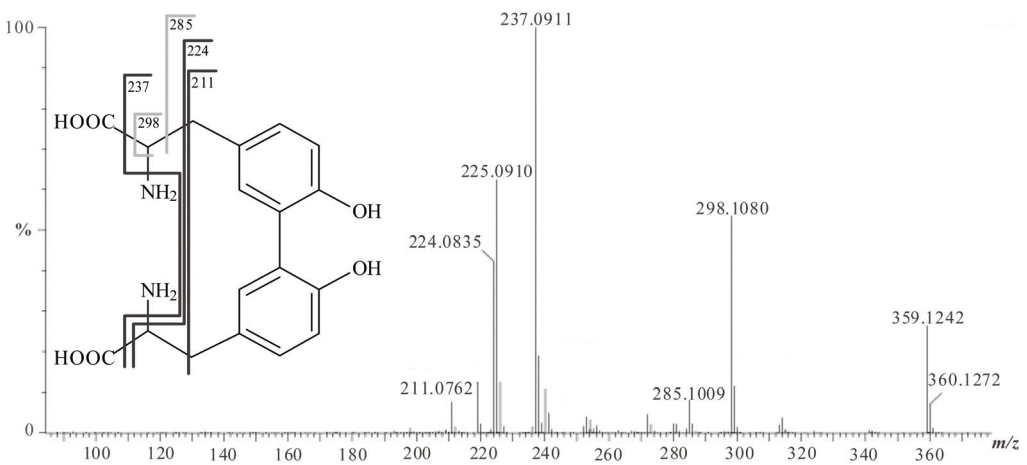

Fig. 5 MS/MS spectrum recorded in ESI^- mode of Tyr_2.

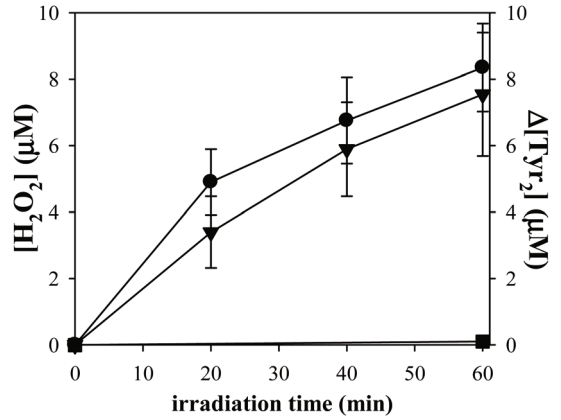

Fig. 6 Time evolution of the H_2O_2 concentration in alkaline (●) and acidic (■) air-equilibrated aqueous solution under UV irradiation, and consumption of Tyr_2 ($\Delta[Tyr_2] = [Tyr_2]_0 - [Tyr_2]_t$) in alkaline medium (▼). $[Tyr_2]_0$ = 14 μM. Alkaline solutions: pH = 9.5, λ_{irr} = 320 nm; acidic solutions: pH = 5.5, λ_{irr} = 280 nm.

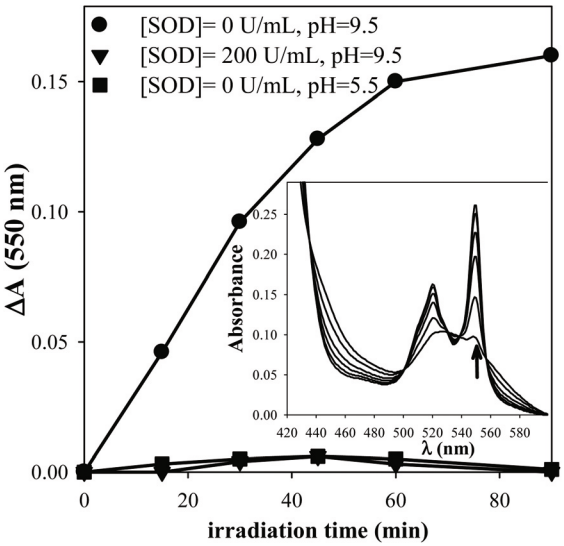

Fig. 7 SOD-inhibitable Cyt reduction assay for the detection of $O_2^{\bullet-}$. Difference absorbance at 550 nm of acidic and alkaline air-equilibrated aqueous solutions containing Cyt c (Fe^{3+}) (14 μM) and Tyr_2 (14 μM) as a function of irradiation time. Alkaline solutions: λ_{irr} = 320 nm; acidic solutions: λ_{irr} = 280 nm. Inset: Time evolution of the absorption spectrum in alkaline air-equilibrated aqueous solution.

In contrast, the concentration of H_2O_2 detected in irradiated acidic solutions was negligible (Fig. 6), which is in agreement with the results shown for the photodegradation of the acid form of Tyr_2. No consumption of Tyr_2 was detected when acid and alkaline aqueous solution of Tyr_2 were stored in the dark in the presence of H_2O_2, thus indicating that no thermal reaction took place between these compounds. On the other hand, control experiments were performed in the absence of O_2, and as expected no H_2O_2 production was observed.

Superoxide anion determination. The H_2O_2 detected can be the product of the spontaneous disproportionation of $O_2^{\bullet-}$, with its conjugate acid $HO_2^{\bullet}$.[38] Therefore, to investigate the formation of $O_2^{\bullet-}$, air-equilibrated aqueous solutions containing 14 μM of Tyr_2 and 14 μM of Cyt at pH 5.5 and 9.5 were irradiated. In alkaline media the difference in the absorbance (ΔA_{550}) increased with irradiation time, reaching a plateau after *ca.* 60 minutes (Fig. 7). The corresponding experimental-difference (ED) spectra in the range 500–600 nm were in good agreement with those reported in the literature for the reduction of Cyt.[39] Photoreduction of Cyt was inhibited in similar experiments performed in the presence of SOD (200 U mL^{-1}), an enzyme that catalyzes the conversion of $O_2^{\bullet-}$ into O_2 and H_2O_2 (Fig. 7). Control experiments were performed to investigate thermal or photochemical processes that might interfere with the assay. No reduction of Cyt was observed in solutions containing 14 μM of Tyr_2 and 14 μM of Cyt at pH 9.5, when kept in the dark for more than 90 min (Fig. S3, ESI†). When solutions containing only Cyt were exposed to UV-A radiation, no changes were observed in the spectra (Fig. S3, ESI†). These results indicated that, under our experimental conditions, $O_2^{\bullet-}$ was generated photochemically by Tyr_2 and provided evidence for the existence of electron transfer reactions.

When the same assay was carried out under acid pH conditions, photoreduction of Cyt was not observed (Fig. 7). This fact is compatible with the results previously shown on photodegradation of Tyr_2 in acidic media, *e.g.* low quantum yield of reactant consumption (Fig. 2) and negligible production of H_2O_2 (Fig. 6).

Singlet oxygen. The production of $^1O_2$ in Tyr_2 solutions was investigated by monitoring its near-infrared (NIR) luminescence at 1270 nm. Due to the weak emission of $^1O_2$ in H_2O, D_2O was used as a solvent and the concentrations of Tyr_2 was higher (165 μM) than that used in the experiments presented up to now. Therefore alkaline solutions (pD = 10.5) were irradiated at 320 nm and NIR corrected emission spectra were recorded. As shown in Fig. 8, the typical phosphorescence spectrum of $^1O_2$ centered at about 1270 nm was observed in air-equilibrated solutions and such emission disappeared when the oxygen was removed from the solution by bubbling with Argon. These results univocally demonstrated that the basic form of Tyr_2 is able to generate $^1O_2$ upon UV-A irradiation.

Controls performed after recording the emission spectra of $^1O_2$ revealed that a significant amount of Tyr_2 was consumed, indicating that the concentration and, consequently, the absorbance at 320 nm, did not remain constant during the NIR emission detection. The Tyr_2 consumption took place in these experiments since the Φ_{-Tyr2} value is high (*vide supra*) and, to improve the weak luminescence detection, the sample was irradiated with a high energy and for a relative long time. Under these conditions, the determination of the quantum yield of $^1O_2$ production (Φ_Δ) by Tyr_2, using emission measurements, would be very difficult and would lead to a very uncertain result.

Therefore the Φ_Δ value in alkaline media was estimated using the probe Singlet Oxygen Sensor Green (SOSG) (Material and methods). Alkaline air-equilibrated aqueous solutions (pH 9.5) of Tyr_2 (14 μM) were irradiated in the presence of SOSG

 This journal is © The Royal Society of Chemistry and Owner Societies 2019

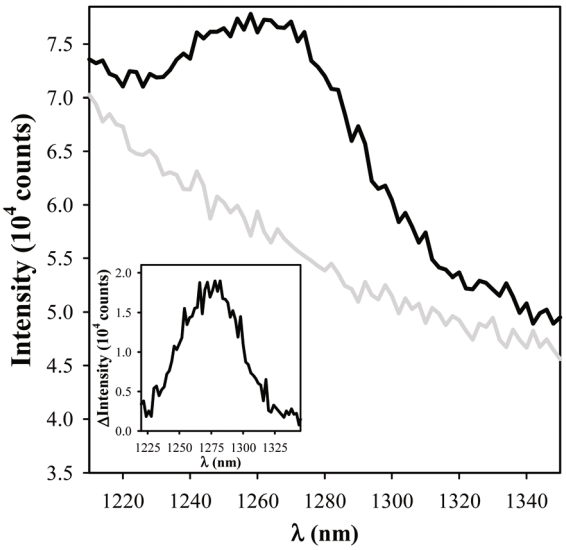

Fig. 8 NIR luminescence of $^1O_2$ photosensitized by Tyr_2 in Argon (gray line) and air-equilibrated D_2O solution (black line) at pD 10.5. Inset: Difference NIR emission spectrum obtained by subtraction of emission spectrum obtained in argon from that obtained in air-equilibrated solution.

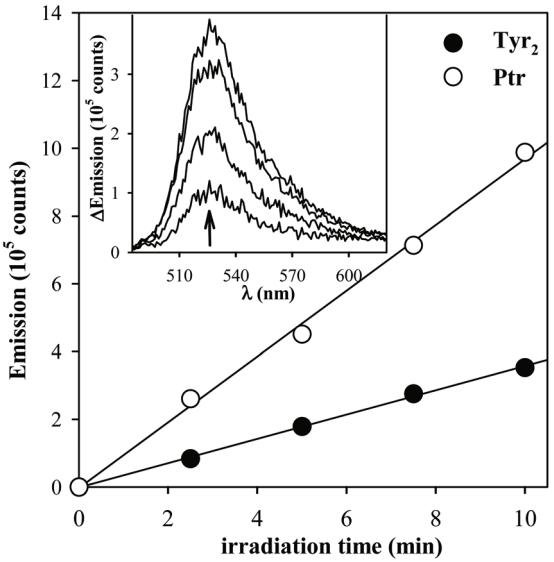

Fig. 9 Evolution of the fluorescence intensity at 525 nm as a function of irradiation time (λ_{irr} = 320 nm) of an alkaline water solution of SOSG in the presence of Tyr_2 ($A_{0(320\ nm)}$ = 0.12, $[Tyr_2]_0$ = 14 μM) and Ptr ($A_{0(320nm)}$ = 0.12, $[Ptr]_0$ = 47 μM). Inset: Corrected fluorescence spectra (λ_{exc} = 470 nm) of SOSG-EP recorded at different times upon irradiation of an alkaline aqueous solution of SOSG and Tyr_2 at 320 nm.

(0.63 mg L^{-1}) and the corresponding emission spectra of the SOSG-EP, upon excitation at 470 nm, were recorded (Material and methods). For each irradiation time, the spectrum before irradiation was subtracted and the resulting difference spectra showed the typical fluorescence band reported for the product of the reaction between SOSG and $^1O_2$ (SOSG-EP)[27–29,40] and its intensity increased with irradiation time (Fig. 9). The time evolution of the fluorescence was registered for Tyr_2 and Ptr, used as a reference (Φ_Δ = 0.30 (alkaline media))[30] (Fig. 9), and Φ_Δ value for Tyr_2, calculated as explained in Material and methods section, was 0.15 ± 0.05.

This value is similar to that obtained for free Tyr (Φ_Δ = 0.138 ± 0.007) upon irradiation in the UV-C, and higher than those reported for others amino acids like Trp and Phe.[37] Therefore, while Tyr is not a relevant $^1O_2$ photosensitizer at physiological conditions because it does not absorb radiation coming from the sun or normal artificial sources, Tyr_2 produces $^1O_2$ with the same quantum efficiency as Tyr, but upon excitation with the mentioned light sources, due to the shift in the absorption spectrum of the Tyr chromophores (Fig. 1).

Degradation of Tyr photoinduced by Tyr_2

Up to now we have shown that Tyr_2, under UV-A irradiation, undergoes photodegradation and produces ROS. Considering this behavior, the next logical step was to evaluate if Tyr_2 is able to act as a photosensitizer of biomolecules. To investigate this issue Tyr was used as an oxidizable substrate. Therefore solutions containing Tyr_2 (15 μM) and Tyr (19.7 μM) (pH = 9.5) were irradiated at 320 nm. Under these conditions only Tyr_2 was excited, whereas Tyr did not absorb. The concentration of reactants was determined by HPLC. As shown in Fig. 10, simultaneously with the expected consumption of Tyr_2, the concentration of Tyr decreased as a function of irradiation time. In a control carried out in the same experimental conditions, but in the absence of Tyr_2, no consumption of Tyr was observed. Similar results were obtained in experiments performed at different Tyr and Tyr_2 concentrations (Fig. S4, ESI†).

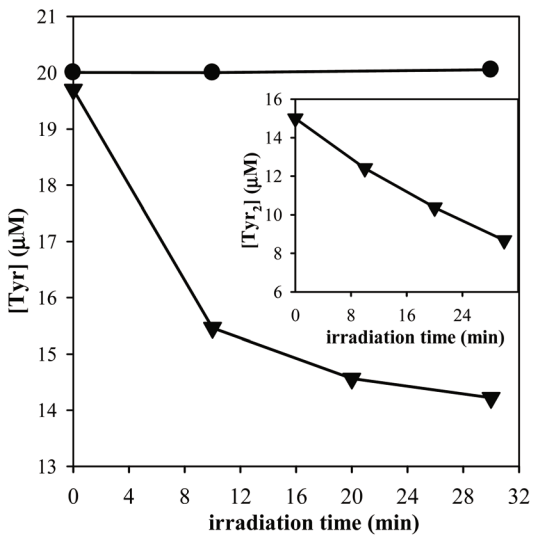

Fig. 10 Time evolution of the Tyr concentration in alkaline aqueous solutions under UV-A irradiation in the absence (●) and in the presence of Tyr_2 (▼). Inset: Time evolution of the Tyr_2 concentrations in alkaline aqueous solutions under UV irradiation in the presence of Tyr. λ_{irr} = 320 nm, [Tyr] = 19.7 μM, $[Tyr_2]$ = 15 μM, pH = 9.5.

These results clearly demonstrated that Tyr is degraded by photosensitization with Tyr_2, indicating that this compound is

able to photoinduced chemical modifications in oxidizable biomolecules. This fact is quite relevant because it means that a compound formed by photosensitization can subsequently act as an intrinsic photosensitizer, amplifying the harmful effects of UV radiation on biological systems.

Conclusions

We have studied the photodegradation of the acid and alkaline form of Tyr_2 in aqueous solution under UV-B and UV-A radiation, considering that both acid–base forms are present at physiological conditions. In the absence of oxygen Tyr_2 is photostable, whereas excitation in the presence of oxygen leads to the photodegradation of Tyr_2. The quantum yield of Tyr_2 photodegradation values are 0.023 ± 0.003 and 0.0053 ± 0.0005 for the alkaline and acid form, respectively. Photolysis of Tyr_2 leads to oxidized products that conserve the dimeric structure, that is the chemical bond between the two Tyr moieties endures the UV exposure.

Reactive oxygen species such as H_2O_2, $O_2^{\bullet-}$ and $^1O_2$ are produced upon excitation of the alkaline form of Tyr_2. The quantum yield of $^1O_2$ production is 0.15 ± 0.05, which is similar to that obtained for free Tyr. Therefore, while Tyr and other aromatic amino acids are not relevant $^1O_2$ photosensitizers because do not absorb radiation coming from the sun or normal artificial sources, Tyr_2 produces $^1O_2$ with the same quantum efficiency as Tyr, but upon excitation with the mentioned light sources, due to the shift in the absorption spectrum of the Tyr chromophore. In addition, we have proven that Tyr_2 is able to photoinduce the degradation of Tyr under UV-A radiation.

The results presented in this work indicate that when Tyr_2 is generated in a protein structure, an intrinsic potential photosensitizer is formed, extending the active fraction of light towards the UVA range. Therefore a product of a photosensitized process can act as a photosensitizer itself leading to further photosensitized damage, thus amplifying the harmful effects of UV radiation on biological systems.

Abbreviations

A	Absorbance
$q^{a,V}_{n,p}$	Absorbed photon flux density
Cyt	Cytochrome c
D_2O	Deuterium water
DOPA	3,4-Dihydroxy-L-phenylalanine
ESI	Electrospray ionization source
I	Emission intensities
ED	Experimental-difference spectra
FL	Fluorescence detector
HCOOH	Formic acid
HPLC	High-performance liquid chromatography
H_2O_2	Hydrogen peroxide
$q^{0,V}_{n,p}$	Incident photon flux densitity
$q^{0}_{n,p}$	Incident photons per time interval
NIR	Near-infrared
Tyr_2	*o*,*o*′-Dityrosine or tyrosine dimer
PDA	Photodiode array detector
Ptr	Pterin
Φ_{-Tyr2}	Quantum yield of tyrosine dimer consumption
ROS	Reactive oxygen species
t_R	Retention times
$^1O_2$	Singlet oxygen
τ_Δ	Singlet oxygen lifetime
SOSG	Singlet oxygen sensor green
SOSG-EP	Singlet oxygen sensor green endoperoxide
Φ_Δ	Singlet oxygen quantum yields
$O_2^{\bullet-}$	Superoxide anion radical
SOD	Superoxide dismutase
Tyr(-H)$^\bullet$	Tyrosyl radical
V	Volume

Conflicts of interest

There are no conflicts to declare.

Acknowledgements

The present work was partially supported by Consejo Nacional de Investigaciones Científicas y Técnicas (CONICET; Grants PIP 0304, PICS No. 05920), Agencia de Promoción Científica y Tecnológica (ANPCyT; Grant PICT 2015-1988), Universidad Nacional de La Plata (UNLP; Grant X712) and Centre National de la Recherche Scientifique (CNRS; Grant PICS No. 05920). L. O. R. thanks CONICET for doctoral research fellowships. We deeply acknowledge Dr Patricia Vicendo for offering her facilities to M. V. and L. O. R during their stays at the Laboratoire des Interactions Moléculaires et Réactivité Chimique et Photochimique (IMRCP), Université Toulouse III (Paul Sabatier), France. The authors thank Dr Matias Rafti for his contributions in the preparation of the Tyr_2 samples. A. H. T., M. V. and M. L. D. are research members of CONICET.

References

1 T. K. Dalsgaard, J. H. Nielsen, B. E. Brown, N. Stadler and M. J. Davies, *J. Agric. Food Chem.*, 2011, **59**, 7939–7947.
2 G. Boguta and A. M. Dancewicz, *Stud. Biophys.*, 1979, **73**, 149–156.
3 G. Boguta and A. M. Dancewicz, *Int. J. Radiat. Biol.*, 1981, **39**, 163–174.
4 R. Amadò, R. Aeschbach and H. Neukom, *Methods Enzymol.*, 1984, **107**, 377–388.
5 K. J. Davies, *J. Biol. Chem.*, 1987, **262**, 9895–9901.

 This journal is © The Royal Society of Chemistry and Owner Societies 2019

6 R. Kanwar and D. Balasubramanian, *Exp. Eye Res.*, 1999, **68**, 773–784.
7 L. O. Reid, E. A. Roman, A. H. Thomas and M. L. Dántola, *Biochemistry*, 2016, **55**, 4777–4786.
8 D. Balasubramanian and R. Kanwar, *Mol. Cell. Biochem.*, 2002, **234/235**, 27–38.
9 L. O. Reid, C. Castaño, M. L. Dántola, V. Lhiaubet-Vallet, M. A. Miranda, M. L. Marin and A. H. Thomas, *Dyes Pigm.*, 2017, **147**, 67–74.
10 S. O. Andersen, *Biochim. Biophys. Acta*, 1963, **69**, 249–262.
11 D. A. Malencik, J. F. Sprouse, C. A. Swanson and S. R. Anderson, *Anal. Biochem.*, 1966, **242**, 202–213.
12 M. Charlier and C. Hélène, *Photochem. Photobiol.*, 1972, **15**, 71–87.
13 T. Delatour, T. Douki, C. D'Ham and J. Cadet, *J. Photochem. Photobiol., B*, 1998, **44**, 191–198.
14 J. Cadet, E. Sage and T. Douki, *Mutat. Res.*, 2005, **571**, 3–17.
15 M. da Silva Baptista, J. Cadet, P. Di Mascio, A. A. Ghogare, A. Greer, M. R. Hamblin, C. Lorente, S. C. Nunez, M. S. Ribeiro, A. H. Thomas, M. Vignoni and T. M. Yoshimura, *Photochem. Photobiol.*, 2017, **93**(4), 912–919.
16 D. I. Pattison, A. S. Rahmanto and M. Davies, *Photochem. Photobiol. Sci.*, 2012, **11**(1), 38–53.
17 E. Silva and J. Godoy, *Int. J. Vitam. Nutr. Res.*, 1994, **64**, 253–256.
18 C. Castaño, M. L. Dántola, E. Oliveros, A. H. Thomas and C. Lorente, *Photochem. Photobiol.*, 2013, **89**, 1448–1455.
19 C. Castaño, E. Oliveros, A. H. Thomas and C. Lorente, *J. Photochem. Photobiol., B*, 2015, **153**, 483–489.
20 A. H. Thomas, M. P. Serrano, V. Rahal, P. Vicendo, C. Claparols, E. Oliveros and C. Lorente, *Free Radical Biol. Med.*, 2013, **63**, 467–475.
21 S. E. Braslavsky, *Pure Appl. Chem.*, 2007, **79**, 293–465.
22 H. J. Kuhn, S. E. Braslavsky and R. Schmidt, *Pure Appl. Chem.*, 2004, **76**, 2105–2146.
23 C. C. Allain, L. S. Poon, C. S. G. Chan, W. Richmond and P. C. Fu, *Clin. Chem.*, 1974, **20**, 470–475.
24 H. M. Flegg, *Ann. Clin. Biochem.*, 1973, **10**, 79–84.
25 J. M. McCord and J. Fridovich, *J. Biol. Chem.*, 1969, **244**, 6049–6055.
26 M. P. Serrano, C. Lorente, C. D. Borsarelli and A. H. Thomas, *ChemPhysChem*, 2015, **16**(10), 2244–2252.
27 A. Gollmer, J. Arnbjerg, F. H. Blaikie, B. W. Pedersen, T. Beitenbach, K. Daasbjerg, M. Glasius and P. R. Ogilby, *Photochem. Photobiol.*, 2011, **87**, 671–679.
28 C. Flors, M. J. Fryer, J. Waring, B. Reeder, U. Bechtold, P. M. Mullineaux, S. Nonell, M. T. Wilson and N. R. Baker, *J. Exp. Bot.*, 2006, **57**, 1725–1734.
29 D. Rodríguez Sartori, C. R. Lillo, J. J. Romero, M. L. Dell'Arciprete, A. Miñan, M. Fernández Lorenzo de Mele and M. C. González, *Nanotechnology*, 2016, **27**, 475–486.
30 C. Lorente and A. H. Thomas, *Acc. Chem. Res.*, 2006, **39**(6), 395–402.
31 I. A. Vladimirov and N. I. Perrase, *Biophysics*, 1966, **11**(4), 578–583.
32 A. Ipiña, C. Castaño, M. L. Dántola and A. H. Thomas, *Solar Energy*, 2014, **109**, 45–53.
33 G. M. Robinson and M. R. Smyth, *Analyst*, 1997, **122**, 797–802.
34 J. R. Lakowicz, *Principles of Fluorescence Spectroscopy*, Springer, New York, 2006, ch. 3.
35 D. Creed, *Photochem. Photobiol.*, 1984, **39**(4), 563–575.
36 J. L. Kerwin, *J. Mass Spectrom.*, 1996, **31**, 1429–1439.
37 K. K. Chin, C. C. Trevithick-Sutton, J. McCallum, St. Jockusch, N. J. Turro, J. C. Scaiano, C. S. Foote and M. A. Garcia-Garibay, *J. Am. Chem. Soc.*, 2008, **130**, 6912–6913.
38 B. H. J. Bielski, D. E. Cabelli, R. L. Arudi and A. B. Ross, *J. Phys. Chem. Ref. Data*, 1985, **14**, 1041–1100.
39 R. Kuciel and A. Mazurkiewicz, *Biochem. Mol. Biol. Educ.*, 2004, **32**, 183–186.
40 S. Kim, M. Fujitsuka and T. Majima, *J. Phys. Chem. B*, 2013, **117**(45), 13985–13992.

This journal is © The Royal Society of Chemistry and Owner Societies 2019